Non-neutral plasma column in an asymmetric trapping field

Sh. Amiranashvili
Department of Theoretical Physics, General Physics Institute, Moscow 119991, Russia

M. Y. Yu
Institut für Theoretische Physik I, Ruhr-Universität Bochum, D-44780 Bochum, Germany

L. Stenflo
Department of Plasma Physics, Umeå University, S-90187 Umeå, Sweden
(Received 14 November 2001; published 14 March 2002)

A non-neutral plasma column in an asymmetric trapping field is considered in this paper. It is shown that nonlinearly interacting bulk plasma oscillations and quadrupole surface waves allow an exact analytical description. The absence of symmetry leads to nonintegrability and other nonlinear phenomena, such as passage through different resonances and phase locking. These phenomena should be observable in experiments involving elliptical traps and rotating walls and can affect the latters' applications.

DOI: 10.1103/PhysRevE.65.046402 PACS number(s): 52.27.Jt, 32.80.Pj, 52.35.Fp

I. INTRODUCTION

A non-neutral plasma can be a collection of identical charges (e.g., ions or electrons) in a trap [1]. The properties of the trapped cloud depend on the plasma density and temperature [2]. Aside from the special case of small Coulomb clusters [3], the size of the cloud can be large compared to the interparticle spacing and the Debye length. Various collective phenomena, such as, plasma waves, have been predicted and observed.

There has been much recent theoretical [4–6] and experimental [7–9] interest in linear electrostatic waves in trapped non-neutral plasmas. These modes are of importance as nondestructive diagnostic tools. They can be easily excited and measured, providing useful information on the plasma shape, size, density, and temperature.

It is well known that the low-order (quadrupole) electrostatic waves in non-neutral plasmas can be described in a mathematically exact manner even in the nonlinear regime [10]. The solutions are exact in the sense that starting from the equations of motion for the cold plasma fluid *no approximation of any kind* (e.g., series expansions or higher-harmonic truncations) needs to be made. It appears that the spatial and temporal dependence of the plasma motion can be separated even in the nonlinear regime. The initial equations are then reduced to a system of ordinary differential equations that can be solved numerically or, in some instances, even integrated [10,11].

Exact solutions of the nonlinear plasma equations are rather rare, and the few cases in which they can be found are consequently rather interesting. Such solutions usually describe particularly simple plasma behavior. They are thus especially suitable as a starting point in understanding the underlying physics of the nonlinearity as well as the study of more complex nonlinear wave interactions. They are useful for verifying various approximations and numerical schemes, and many of such solutions can also be used directly to explain observed phenomena or indirectly for the diagnostics of the plasma.

An equilibrium state of a non-neutral plasma in a harmonic trap is the uniform ellipsoid [12,13]. The space charge electric field within a uniformly charged ellipsoid is a linear function of the position. A key feature of the quadrupole modes is that the plasma conserves the ellipsoidal form and consequently the linear spatial dependence of the electric field. Nonlinear surface waves with the same structure were recently found for plasmas bounded by a dielectric [14–16]. Originally, such solutions were investigated in connection with the gravitating fluid equilibrium [17]. The analogy is expected, since both systems have the inverse square law of the interparticle force, whose field satisfies the Poisson equation.

II. BASIC EQUATIONS

In this paper we investigate linear and nonlinear oscillations in a non-neutral plasma cylinder. That is, the equilibrium ellipsoid is here highly elongated in the z direction. The particles are assumed to be trapped in the external potential field

$$U_{\mathrm{ext}}=\tfrac{1}{2}m(\omega_1^2x^2+\omega_2^2y^2),$$

where m is the particle mass, and $\omega_{1,2}$ are the frequencies of the transverse oscillations. The transverse plasma size is small as compared to the distance between the trap electrodes, so that U_{ext} is quadratic in terms of the Taylor expansion.

In contrast to earlier investigations of trapped-plasma oscillations the trapping field has no rotational symmetry. An elliptical Paul trap [18] is an example of such asymmetry. In a Penning trap a time-independent asymmetric trapping potential can exist in a frame rotating with the plasma, as was observed in a recent experiment involving a rotating wall [2].

We also assume that the plasma is unmagnetized, as in the Paul trap. For the Penning trap our results can be applied only in the case of ''Brillouin flow'' when the plasma is

compressed to its maximum density [1], since in the rotating frame the plasma behaves like an unmagnetized one.

We describe the trapped plasma by the standard cold-fluid model, i.e., the velocity $\mathbf{v}$ satisfies the pressureless Euler equation

$$\frac{\partial \mathbf{v}}{\partial t}+(\mathbf{v}\cdot\boldsymbol{\nabla})\cdot\mathbf{v}=\frac{q}{m}\mathbf{E}-\frac{1}{m}\boldsymbol{\nabla}U_{\mathrm{ext}}, \tag{1}$$

where the space charge electric field is purely electrostatic: $\mathbf{E}=-\boldsymbol{\nabla}\varphi$, and φ obeys the Poisson equation

$$\nabla^2\varphi=-4\pi qn, \tag{2}$$

where q is the charge of the trapped particles. To close the system we have the continuity equation

$$\frac{\partial n}{\partial t}+\boldsymbol{\nabla}\cdot(n\mathbf{v})=0, \tag{3}$$

where n is the density.

For the Paul trap these equations can be applied directly, whereas for the Penning trap they are valid in the rotating frame. In this paper the analysis will be limited to two dimensions. We shall investigate the plasma equilibrium state, linear waves as well as exact nonlinear oscillations.

III. LINEAR WAVES

We start with the description of the equilibrium state. Earlier investigations [12,13] showed the existence of an ellipsoidal equilibrium. It can be easily verified that an immobile plasma can form a uniform cylinder with elliptical cross section,

$$\frac{x^2}{a_0^2}+\frac{y^2}{b_0^2}=1,$$

and $n=n_0$. The space charge electric field within such a cylinder is linear [17] and the corresponding potential is

$$\varphi=\pi qn_0(\mathrm{const}-A_1x^2-A_2y^2), \tag{4}$$

where $A_1=2b_0/(a_0+b_0)$ and $A_2=2a_0/(a_0+b_0)$.

For a steady-state ($\mathbf{v}=\mathbf{0}$) equilibrium, Eqs. (1)–(3) are reduced to the condition $\boldsymbol{\nabla}(q\varphi+U_{\mathrm{ext}})=0$. Thus we get [2]

$$\tfrac{1}{2}\omega_p^2A_1=\omega_1^2 \quad \text{and} \quad \tfrac{1}{2}\omega_p^2A_2=\omega_2^2,$$

where $\omega_p=(4\pi q^2n_0/m)^{1/2}$ is the plasma frequency. The condition

$$\omega_1^2+\omega_2^2=\omega_p^2 \tag{5}$$

thus uniquely determines the plasma density.

It is convenient to denote the number of particles per unit column length by the free parameter N of the system. Accordingly we can introduce the quantity

$$R=\sqrt{\frac{N}{\pi n_0}},$$

which represents the typical radius of the plasma column. The equilibrium values of the semiaxes are then

$$a_0=\frac{\omega_2}{\omega_1}R \quad \text{and} \quad b_0=\frac{\omega_1}{\omega_2}R, \tag{6}$$

and without loss of generality we can assume $\omega_1<\omega_2$, so that $a_0>b_0$.

Apart from the steady-state equilibrium, there are many general dynamic equilibria with $\mathbf{v}\neq\mathbf{0}$. For instance, the plasma can rotate within the elliptical boundary. Leaving aside these more complicated cases, we can describe the plasma waves in terms of a dielectric tensor ε_{ij}. For studying linear electrostatic waves one has then only to solve the equation $\partial_i(\varepsilon_{ij}\partial_j\delta\varphi)=0$ for the perturbed electric potential and apply the appropriate boundary conditions.

In our model the plasma is described by the cold-plasma dielectric tensor $\varepsilon_{ij}=(1-\omega_p^2/\omega^2)\delta_{ij}$, so that the perturbed potential inside and outside the plasma obeys the Laplace equations

$$\left(1-\frac{\omega_p^2}{\omega^2}\right)\nabla^2\delta\varphi_{in}=0 \quad \text{and} \quad \nabla^2\delta\varphi_{out}=0,$$

whereas the boundary conditions on the plasma surface S are

$$\delta\varphi_{in}|_S=\delta\varphi_{out}|_S, \quad \left(1-\frac{\omega_p^2}{\omega^2}\right)\frac{\partial}{\partial\mathbf{n}}\delta\varphi_{in}|_S=\frac{\partial}{\partial\mathbf{n}}\delta\varphi_{out}|_S,$$

where $\mathbf{n}$ is a unit vector normal to S.

One solution is $\omega^2=\omega_p^2$ and $\delta\varphi_{out}=0$. This corresponds to bulk plasma oscillations with arbitrary $\delta\varphi_{in}$ related to some density variation δn. The only restriction is that the plasma perturbation causes no change in the external potential. For example, the plasma cylinder can oscillate at the plasma frequency in a self-similar manner. We will consider such a mode in the following section.

For the other solution the plasma density is unperturbed and $\delta\varphi$ is a harmonic function. A comprehensive study of the Laplace equation for an elliptical cylinder requires Mathieu functions [19]. This will be considered elsewere, and here we restrict ourselves to the simple case of transverse two-dimensional (2D) oscillations with $\delta\varphi=\delta\varphi(x,y)$. The plasma configuration suggests the use of elliptic coordinates $\xi\in(0,\infty)$ and $\eta\in(0,2\pi)$, satisfying $x=c\cosh\xi\cos\eta$ and $y=c\sinh\xi\sin\eta$, where c is, in general, a free parameter. Setting $c=\sqrt{a_0^2-b_0^2}$ makes the plasma boundary a surface of constant $\xi=\xi_0$, where

$$\xi_0=\frac{1}{2}\ln\frac{a_0+b_0}{a_0-b_0}.$$

The coordinate system (ξ,ν) is conformal so that the Laplace operator in the new system is proportional to $\partial^2/\partial\xi^2+\partial^2/\partial\eta^2$. The corresponding harmonic functions are

readily obtained. An important restriction is that the electric field $\delta\mathbf{E}=-\nabla\delta\varphi$ should be finite at the ellipse focuses (e.g., the critical points of the coordinate system). The solution inside the elliptic plasma cylinder can then be written as

$$\delta\varphi_{in}=c_1\cosh m\xi\cos m\eta+c_2\sinh m\xi\sin m\eta,$$

where c_1 and c_2 are constants. Here the positive integer m plays the role of the azimuthal wave number. Outside the plasma, we have

$$\delta\varphi_{out}=c_3\exp(-m\xi)\cos m\eta+c_4\exp(-m\xi)\sin m\eta,$$

because of the condition $\delta\varphi_{out}\to 0$ at large distances. Here c_3 and c_4 are constants.

Applying the boundary conditions at $\xi=\xi_0$, we obtain the following spectrum:

$$\omega^2=\frac{1}{2}\omega_p^2\left[1\pm\left(\frac{a_0-b_0}{a_0+b_0}\right)^m\right],\quad m\geqslant 1 \tag{7}$$

for the oscillations.

There are two discrete series of frequencies. For $a_0=b_0$ the spectrum reduces to the familiar relation $\omega=\omega_p/\sqrt{2}$ for the electrostatic surface oscillations. Taking $a_0\to\infty$, $m\to\infty$ and $k=m/a_0=\text{const}$, one can also reproduce the spectrum $\omega^2=(1/2)\omega_p^2[1\pm\exp(-2kb_0)]$ of surface waves in an infinite plasma layer.

Using the expressions (6) for the semiaxes along with Eq. (5) for the plasma frequency one can rewrite the spectrum in terms of the trapping parameters. In particular, the frequencies with $m=1$ are identical to the trap frequencies $\omega_{1,2}$. These modes correspond to the center-of-mass motion of the column.

The potential $\delta\varphi_{in}$ corresponding to the quadrupole $m=2$ modes is a quadratic function of the Cartesian coordinates. It follows that the deformed plasma column has also an elliptical cross section, but generally with different orientation and time varying semiaxes. These oscillations can be described exactly even in the nonlinear regime. The higher modes with $m>2$ involve significant changes of the plasma shape and potential.

It should be mentioned that Eq. (7) does not cover all the possible plasma modes. There are still perturbations that do not involve the potential nor plasma surface motion. For example, we can consider a velocity perturbation of the form

$$v_x=-\Omega\frac{a}{b}y,\quad v_y=\Omega\frac{b}{a}x,$$

where Ω is infinitesimal and generally depends on z. The perturbed plasma rotates within an elliptical boundary. The frequency of such torsion modes is identically zero in the cold-fluid model. Here the restoration forces are from the correlation between the particles.

IV. A NONLINEAR SOLUTION

In this section we discuss an exact nonlinear solution representing two coupled plasma modes. This is described by the full system (1)–(3) and an additional equation for the plasma boundary [17]

$$\frac{\partial S}{\partial t}+(\mathbf{v}\cdot\nabla)S=0, \tag{8}$$

where $S(\mathbf{x},t)$ is arbitrary and the boundary is determined by the relation $S(\mathbf{x},t)=\text{const}$. We assume that the size of the trapped cloud is large compared to the Debye length, so that the plasma can be considered to have a sharp boundary [20].

We assume that the perturbed plasma is uniform, $n=n(t)$, and has an elliptic cross section with the same orientation of the semiaxes. Thus, we have

$$S(\mathbf{x},t)=\frac{x^2}{a^2}+\frac{y^2}{b^2},$$

where the time-dependent semiaxes $a(t)$ and $b(t)$ are unknown. The plasma velocity is chosen to be

$$v_x=\frac{\dot a}{a}x,\quad v_y=\frac{\dot b}{b}y,$$

in accordance with the predefined elliptic shape. Here the overdots denote time derivatives. The given plasma behavior can be considered as ansätz for solving Eqs. (1)–(3) and Eq. (8). It is easy to see that Eq. (8) is satisfied identically, and the continuity equation results in $d(nab)/dt=0$ so that particle density is

$$n(t)=\frac{R^2}{ab}n_0,$$

and the solution of the Poisson equation is of a similar structure as in Eq. (4), but with time-dependent density and semiaxes.

Finally, it is easy to verify that Eq. (1) leads to two ordinary differential equations for the semiaxes

$$\ddot a+\omega_1^2 a=\omega_p^2\frac{R^2}{a+b},\quad \ddot b+\omega_2^2 b=\omega_p^2\frac{R^2}{a+b}, \tag{9}$$

where the value of ω_p is given by expression (5).

The system (9) provides a complete description of two coupled nonlinear modes. Although it is rather simple, it is nevertheless nonintegrable. Aside from the two trivial cases of a circular column and an infinite plasma layer, the system is associated to chaotic dynamics.

We shall first consider the basic properties of Eqs. (9). There is one fixed point of the motion, given by Eq. (6). It is always stable and corresponds to an equilibrium column. Considering small oscillations around this point, one can immediately obtain the linear limit of the two modes. One mode corresponds to oscillations with $a^2-b^2=\text{const}$, so that the plasma oscillates in a self-similar manner without any perturbation of the external field. It is the bulk wave at the plasma frequency as mentioned above. For the second mode

we have $ab=\text{const}$, so that the density remains unperturbed. This mode can be recognized as the lower of the two quadrupole $m=2$ modes.

In general, we still have the bulk and quadrupole surface oscillations. However, in the nonlinear regime they are coupled. Nevertheless, in two simple limiting cases the problem can still be solved by direct integration. For $\omega_1=\omega_2$ we have an axially symmetric trapping field. Equations (9) are then clearly integrable. In fact, the quadrupole dynamics of the non-neutral plasma column in an axially symmetric trapping field is an integrable problem under much more general conditions [21]. In particular, for $\omega_{1,2}=0$ we have a 2D version of the Coulomb expansion [22]. The other simple limiting case is a plasma layer in a one-dimensional trapping field. This limit is obtained by keeping $\omega_1\to 0$, $R\to\infty$, so that $b_0=\text{const}$. Then we have $a_0\to\infty$ and the plasma is trapped in the region $|y|<b_0$. The equation for the layer thickness takes the limiting form $\ddot{b}+\omega_2^2 b=\omega_p^2 b_0$ along with the new condition $\omega_2=\omega_p$ for the plasma density. The boundary of the layer oscillates at the plasma frequency. Note that the plasma density is proportional to $1/b$ and behaves in a nonlinear manner. Similar exact one-dimensional oscillations of a plasma layer have been considered earlier [23]. Note, that for large amplitudes $b(t)$ is negative, whereas $n(t)$ passes through an infinite value. Such unphysical behavior is related to the neglect of the pressure forces. This occurs also in 2D and 3D [10]. Consequently, Eqs. (9) are not valid for very large amplitudes.

V. NON-INTEGRABLE DYNAMICS

In this section we investigate numerically the coupled nonlinear modes. From here on we will use dimensionless variables. The time is normalized by $1/\omega_p$ and the distance by R. We also introduce the parameter

$$\delta=\frac{\omega_2^2-\omega_1^2}{\omega_1^2+\omega_2^2}$$

describing the anisotropy of the trap. Finally, we pass to the variables $u=a+b$ and $v=a-b$ in Eqs. (9) to obtain

$$\ddot{u}+\frac{1}{2}u-\frac{2}{u}=\frac{\delta}{2}v,\quad \ddot{v}+\frac{1}{2}v=\frac{\delta}{2}u, \tag{10}$$

where $\delta\in(0,1)$. The equilibrium point is

$$u_0=\frac{2}{\sqrt{1-\delta^2}},\quad v_0=\frac{2\delta}{\sqrt{1-\delta^2}},$$

and the linear frequencies take the form

$$\omega_b=1,\quad \omega_q=\sqrt{(1-\delta^2)/2}, \tag{11}$$

where ω_b and ω_q are for the bulk and quadrupole modes, respectively. An important *resonance condition* is met when the ratio ω_b/ω_q of the frequencies is a rational number [24]. Even in the linear approximation it is clear that for specific values of δ different resonances can occur. We will especially be interested in the low-order resonances, of the form 3:2 for $\delta=1/3$ and 2:1 for $\delta=1/\sqrt{2}$.

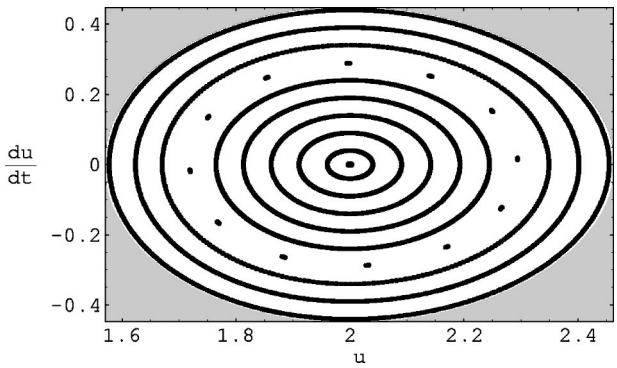

FIG. 1. A Poincaré surface of section for motions corresponding to bulk and quadrupole modes with $H=0.1$ and $\delta=0$. The system is integrable, nested curves represent orbits on different tori. The discrete set of points corresponds to a 17:12 resonance orbit. The point at the center represents the pure quadrupole surface mode. The pure bulk mode corresponds to an orbit that surrounds the whole plot.

For $\delta=0$, Eqs. (10) describe two independent oscillators, but there is no simple way to solve the problem for $\delta\neq 0$. On the other hand, the existence of resonances suggests that the dynamics can be complicated. Thus we shall consider Eqs. (10) more carefully. First, we note that the set (10) has a Hamiltonian

$$H=\frac{1}{2}(\dot{u}^2+\dot{v}^2)+\frac{1}{4}(u^2-2\delta uv+v^2)+2\ln\frac{u_0}{u}-1, \tag{12}$$

where the constant was chosen such that $H=0$ at equilibrium.

The four-dimensional phase space of the system (10) is reduced to three dimensions by the condition $H=\text{const}$. A key question is whether an independent second integral exists. If it does, the system would then be integrable and the phase curves lie on two-dimensional tori. A traditional way to investigate the problem is to choose a 2D surface in the phase space and construct a map of intersections of the phase trajectory with the surface. Treating numerically the different trajectories we obtain a *Poincaré map* [25,26].

If the system is integrable, the points would represent the intersection of the tori with the 2D surface and they would form smooth closed curves. In general, with sufficiently long integration time, most curves seem to be continuous. All orbits on each torus are characterized by two frequencies, namely, ω_b and ω_q given by Eqs. (11) in the linear limit. On the other hand, even for ''infinite'' integration time some orbits appear as a markedly discrete set of points on the surface of the section. They correspond to resonance tori. With perturbations the resonance tori can be destroyed, providing the ''seeds'' of chaotic behavior observed in nonintegrable systems.

A series of maps with different values of δ is presented in Figs. 1–5. All trajectories have the same energy $H=0.1$.

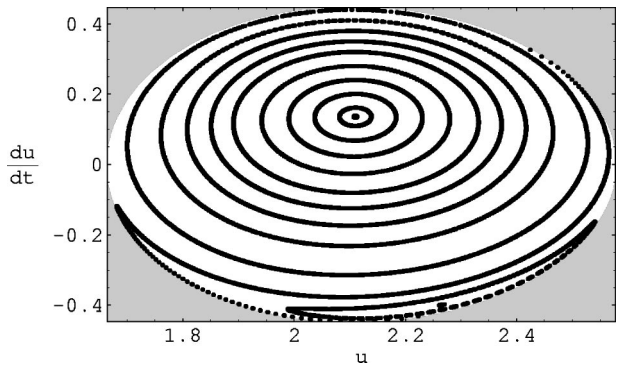

FIG. 2. Surface of section for $H=0.1$ and $\delta=0.32$. Qualitatively it is close to that of Fig. 1, but here both periodic orbits arising from the quadrupole surface and the bulk oscillations can be seen. Due to nonlinear coupling it is impossible to describe these orbits analytically.

Note that the Hamiltonian (12) supports bounded motion, so that only a finite region on the surface of the section is occupied. The excluded region is shaded. The surface of the section is chosen to be $v=0.95v_0$ and the coordinates on that are plane $(u,\dot{u})$. We have mapped only intersections with $\dot{v}>0$, so that each point uniquely represents the state of the system.

A typical map for the integrable case $\delta=0$ is presented in Fig. 1. We see a series of nested closed curves representing different tori. The circles surround a point representing a periodic orbit with only the quadrupole mode excited. Another important periodic orbit corresponds to the pure bulk mode. This orbit happens to lie directly on the surface of the section (the ''last'' curve). We will see that for $\delta\neq 0$ both periodic orbits survive and are represented by points.

The other orbits are quasiperiodical with two frequencies ω_b and ω_q. The former has a nonlinear shift so that the ratio ω_b/ω_q varies from torus to torus. Thus the system obeys the condition of *isoenergetic nondegeneracy*, and when perturbed will be subject to the KAM theorem [25]. When the ratio ω_b/ω_q passes through a rational value we have a periodic orbit corresponding to the particular resonance. For small energies this ratio is close to its linear value so that all

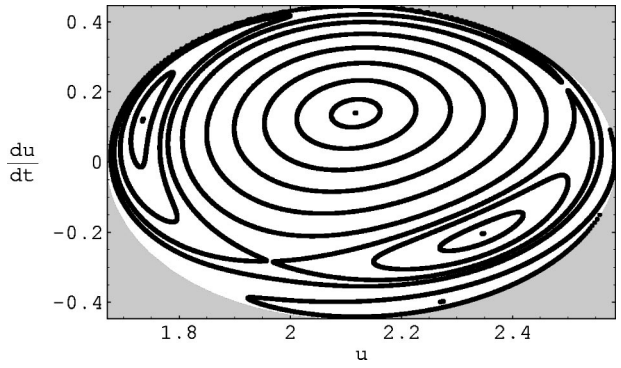

FIG. 3. Surface of section for $H=0.1$ and $\delta=0.33$. The significant difference from Fig. 2 is due to the appearance of the low-order 3:2 resonance torus. That torus is broken, giving rise to elliptical and hyperbolical points.

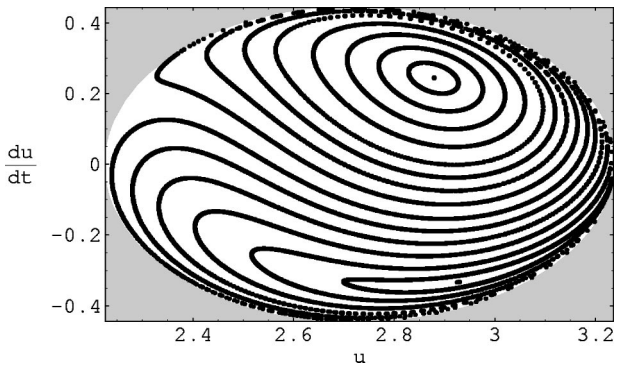

FIG. 4. Surface of section for $H=0.1$ and $\delta=0.69$. Qualitatively there is no difference with Fig. 2.

resonances correspond to rational approximations to $\sqrt{2}$. We found and displayed the lowest 17:12 resonance orbit. Recall that resonance tori can occur as frequently as rational numbers among irrationals, but here only the lowest resonance corresponding to our particular values of energy and δ is displayed.

We now consider the perturbed system with $\delta\neq 0$. In accordance with the KAM theorem most nonresonant tori are conserved and the corresponding orbits stay quasiperiodical as long as δ is small. Note, that all existing resonance orbits are of high order, so that for $\delta\ll 1$ the system can be successfully described by means of perturbation theory. For example, a Poincaré plot for $\delta=0.32$ (Fig. 2) is essentially the same as that for $\delta=0$, the only difference being that now both periodic orbits can be seen.

As mentioned, the ratio ω_b/ω_q is different for each torus and is determined nonlinearly. Nevertheless, the linear expressions (11) suggest that this ratio generally increases with δ, so that resonances disappear and appear. For infinitesimal values of the energy this happens only for a discrete set of δ. For example, the resonance displayed in Fig. 1 should be observed only for $\delta=1/17$. Of course, the nonlinear frequency shift can change this behavior and each resonance can exist in some interval of δ. These intervals increase with the energy, giving rise to resonance overlapping and chaos.

The low-order resonance tori are of special interest, because when perturbed they capture a significant part of the

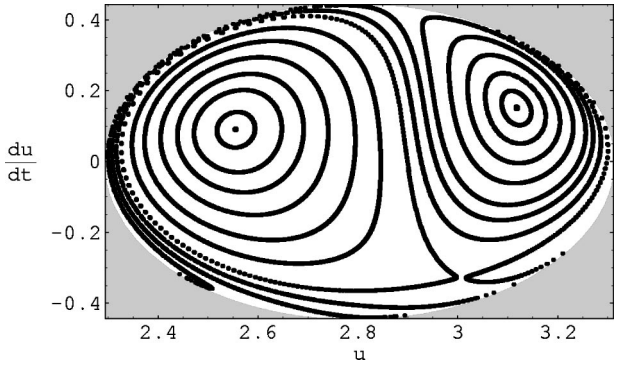

FIG. 5. Surface of section for $H=0.1$ and $\delta=0.71$. Again there is a low-order resonance. It is responsible for the appearance of the unstable hyperbolic point.

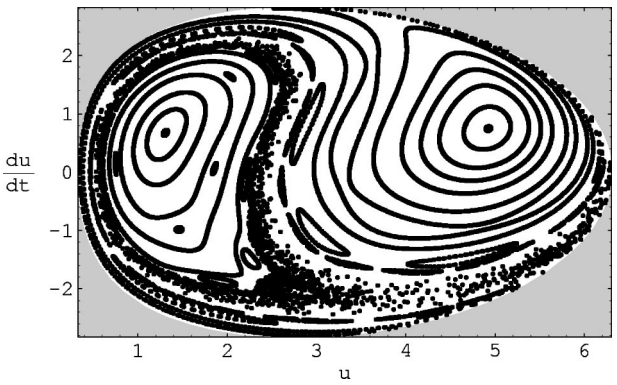

FIG. 6. Surface of section for $H=4$ and $\delta=1/\sqrt{2}$. Periodical orbits remain, with the surrounding stable islands, but now they are separated by stochastic regions.

phase space. Let us now consider the low order 3:2 resonance torus, which arises for δ close to 1/3.

Figure 3 shows the surface of the section for $\delta=0.33$. The resonance comes into being and the map is significantly changed compared to Fig. 2. The resonance torus is destroyed giving rise to a typical chain of elliptic and hyperbolic fixed points [26]. Trajectories jump successively from island to island, gradually filling up the set of two closed curves around the elliptic points. The entire captured area of the surface of the section imitates the same 3:2 repeating pattern as the initial periodic orbit (phase locking). For $\delta=0.34$ the resonance disappears and the surface of the section (not shown) is similar to Fig. 2.

Another low-order 2:1 resonance exists for δ close to $1/\sqrt{2}$. Figures 4 and 5 show the surface of the section for $\delta=0.69$ and $\delta=0.71$, respectively. Again the map is significantly changed with the birth of an unstable hyperbolic point. This resonance disappears for $\delta=0.73$. A passage of our system through other resonances can also be observed. The open (S-like) and even broken (into two parts) curves appear in Figs. 4 and 5 due to the condition $\dot{v}>0$ in the construction of the surface of the section. Only closed curves will appear if one displays *all* orbit intersections with the surface of the section. Another notable feature is the existence of stable periodical orbits represented by isolated points for all values of δ. They give way to isolated islands of regular motion in a sea of chaotic behavior as the energy increases.

Thus the phase space dynamics is regular when the tori are intact, and exhibits features, such as, resonances and phase locking, as is typical for *soft chaos* [27]. With increasing energy a typical sea of chaotic behavior is obtained. This is illustrated in Fig. 6 with $\delta=1/\sqrt{2}$ and $H=4$. A significant part of the surface of the section is filled by a random splatter of points (generated by a single orbit). In this region the behavior of the system is clearly chaotic. A similar transition to chaos was also observed for other values of δ.

The results on transition to chaos, such as that in Fig. 6, should be taken cautiously. All the chaotic regimes were obtained at a high value of the energy. For such energies the semiaxes can permanently change sign during the evolution, as was pointed out at the end of the preceding section. For these regimes, pressure effects, neglected in the initial equations, are important. In fact, all physically meaningful regimes described by Eqs. (10) are regular, corresponding only to soft chaos onset. Nevertheless, a variety of notable phenomena typical for nonintegrable systems, such as, passage through resonances and phase locking, are observed.

VI. CONCLUSION

We have analyzed the nonlinear equations describing a non-neutral plasma column in an electromagnetic trap. A key feature of the trapping field is the absence of rotational symmetry, as in the elliptical Paul trap. Our results are also applicable to the Penning trap with a rotating wall. The equilibrium plasma column has an elliptical cross section. An analytical form for the spectrum of the transverse plasma oscillations exists. The frequencies depend on the trap parameters, plasma form, and density. Thus, our results can be useful for explaining phenomena occurring in non-neutral plasmas as well as the diagnostics of the latter. A fully nonlinear description of the low-order modes is possible. The equations for the cold plasma fluid can be expressed in terms of two simple ordinary differential equations for the bulk and the quadrupole surface modes. The set is found to be nonintegrable. No regime with widespread chaos was found for the present pressureless plasma model. Nevertheless, other important features typical for quasiregular nonintegrable systems exists. These features include the birth and decay of resonances, collapse of corresponding resonance tori, phase locking, and existence of islands surrounding stable periodical orbits. All these nonlinear phenomena should be observable in experiments involving asymmetric trapping fields. In particular, we found that in the neighborhood of resonances a significant change of the plasma behavior is caused by small changes in the anisotropy of the trap. For moderate energies all resonances are accurately predicted by the linear expressions for the frequencies.

ACKNOWLEDGMENTS

This work was partially supported by the Sonderforschungsbereich 191. One of the authors (S.A.) would like to thank the Humboldt Foundation for financial support and A.M. Ignatov for useful discussions.

[1] R. C. Davidson, *Physics of Non-Neutral Plasmas* (Addison-Wesley, Redwood City, 1990).
[2] D.H.E. Dubin and T.M. O'Neil, Rev. Mod. Phys. **71**, 87 (1999).
[3] H. Walther, Adv. At., Mol., Opt. Phys. **31**, 137 (1993).
[4] D.H.E. Dubin, Phys. Rev. Lett. **66**, 2076 (1991).
[5] D.H.E. Dubin and J.P. Schiffer, Phys. Rev. E **53**, 5249 (1996).
[6] D.H.E. Dubin, Phys. Rev. E **53**, 5268 (1996).

[7] D.J. Heinzen, J.J. Bollinger, F.L. Moore, W.M. Itano, and D.J. Wineland, Phys. Rev. Lett. **66**, 2080 (1991).
[8] J.J. Bollinger, D.J. Heinzen, F.L. Moore, W.M. Itano, D.J. Wineland, and D.H.E. Dubin, Phys. Rev. A **48**, 525 (1993).
[9] M.D. Tinkle, R.G. Greaves, C.M. Surko, R.L. Spencer, and G.W. Mason, Phys. Rev. Lett. **72**, 352 (1994).
[10] D.H.E. Dubin, Phys. Fluids B **5**, 295 (1993).
[11] Sh.G. Amiranashvili, Phys. Rev. E **62**, 1215 (2000).
[12] J.H. Malmberg and T.M. O'Neil, Phys. Rev. Lett. **39**, 1333 (1977).
[13] L. Turner, Phys. Fluids **30**, 3196 (1987).
[14] L. Stenflo and M.Y. Yu, Phys. Rev. A **42**, 4894 (1990).
[15] L. Stenflo, M.Y. Yu, and S.V. Vladimirov, Phys. Rev. E **48**, 4859 (1993).
[16] L. Stenflo and M.Y. Yu, Phys. Rev. E **51**, 1408 (1995).
[17] S. Chandrasekhar, *Ellipsoidal Figures of Equilibrium* (Yale University Press, New Haven, 1969).
[18] R.G. DeVoe, Phys. Rev. A **58**, 910 (1998).
[19] G. Blanch, in *Handbook of Mathematical Functions*, Natl. Bur. Stand. Appl. Math. Ser. No. 55, edited by M. Abramowitz and A. Stegun (U.S. GPO, Washington, D.C., 1964).
[20] S.A. Prasad and T.M. O'Neil, Phys. Fluids **22**, 278 (1979).
[21] Sh.G. Amiranashvili, Plasma Phys. Rep. **25**, 846 (1999).
[22] V.A. Levi, J. Appl. Mech. Tech. Phys. **2**, 122 (1967).
[23] L. Stenflo, Phys. Scr. **63**, 59 (1996).
[24] L.D. Landau and E.M. Lifshitz, *Mechanics* (Pergamon Press, Oxford, 1976).
[25] V.I. Arnold, *Mathematical Methods of Classical Mechanics* (Springer-Verlag, New York, 1978).
[26] M. Tabor, *Chaos and Integrability in Nonlinear Dynamics: An Introduction* (Wiley, New York, 1989).
[27] M.C. Gutzwiller, *Chaos in Classical and Quantum Mechanics* (Springer-Verlag, New York, 1990).